11 WCEE
*Paper No. 2082. (quote when citing this article)*
Eleventh World Conference on Earthquake Engineering
ISBN: 0 08 042822 3

# LOCAL SOIL CONDITION AND NONLINEAR FE MODEL

HENG-YIH CHAO and RONALDO I. BORJA

Department of Civil Engineering, Stanford University
Stanford, CA 94305-4020, USA

## ABSTRACT

Foundations are designed to resist seismic loads, which could be influenced significantly by local soil conditions. This paper describes a fully nonlinear finite element model for investigating the effect of local soil condition on the ground response to seismic shaking. The model is tested against a free-field downhole motion recorded by an array at a Large-Scels Seismic Test site in Lotung, Taiwan, during the earthquake of May 20, 1986. Results of the analysis underscore the importance of hysteretic and viscous soil behavior on the predicted nonlinear ground response.

## KEYWORDS

Finite element method; nonlinear analysis; plasticity; site amplification; soil-structure interaction; structural dynamics; time-domain analysis.

## INTRODUCTION

Nonlinear ground response analyses are conventionally carried out by the equivalent linear method (Seed and Idriss 1969; Schnabel et al. 1972; Kausel and Roësset 1984; Chang et al. 1990). In this method, approximate linear solutions are obtained iteratively by assuming constant values of soil properties during the earthquake, but these properties are chosen according to the strain levels predicted from the previous iteration. This method works well for one-dimensional wave propagation problems, but could be difficult to implement in a three-dimensional setting. Since nonlinear wave propagation problems are essentially three-dimensional in nature because of plastic coupling effects even if all wave components propagate in the same direction, difficulties will generally arise when nonlinear ground response analysis is carried out by the equivalent linear method.

This paper presents a fully nonlinear finite element (FE) model for ground response analysis incorporating the three-dimensional plastic coupling effects. The formulation collapses neatly to well-known one-dimensional wave propagation models in the limit of uncoupled responses, but the analysis remains fully nonlinear in the time domain. A key ingredient of the FE model is a 3D bounding-surface plasticity theory with a vanishing elastic region, which allows the three components of motion to be coupled

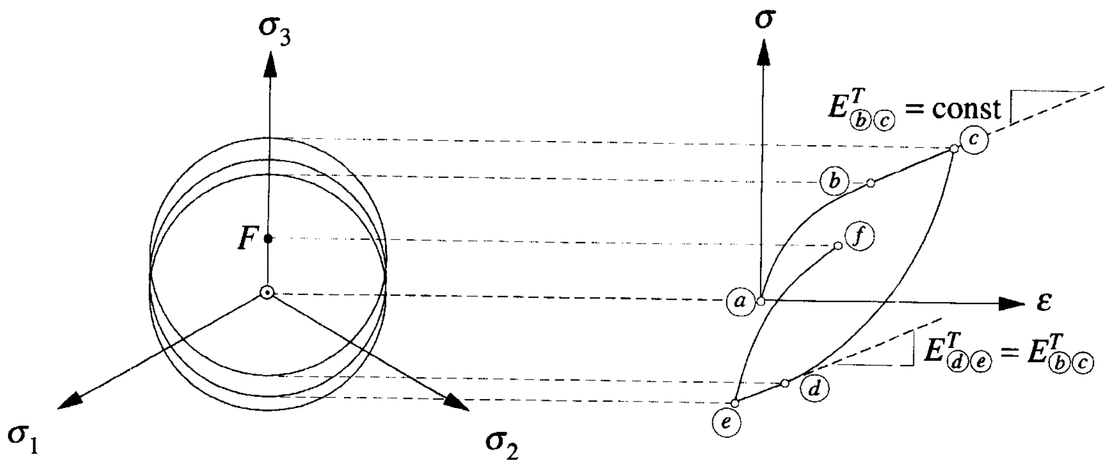

Figure 1. Schematics of bounding surface plasticity model on $\pi$-plane.

naturally in the solution. In the limit of one-dimensional wave propagation, the model automatically captures the shear stiffness degradation and damping ratio variation with shear strain, but the algorithm remains fully nonlinear. The model is tested against a free-field downhole motion recorded by an array at a Large-Scale Seismic Test (LSST) site in Lotung, Taiwan, during the earthquake of May 20, 1986.

## FINITE ELEMENT MODEL

The integrated FE equation of motion takes the form

$$\boldsymbol{M}\boldsymbol{a}_{n+1} + (1+\alpha)\boldsymbol{C}\boldsymbol{v}_{n+1} - \alpha\boldsymbol{C}\boldsymbol{v}_n + (1+\alpha)\boldsymbol{F}_{INT}(\boldsymbol{\sigma}_{n+1}) - \alpha\boldsymbol{F}_{INT}(\boldsymbol{\sigma}_n) = \boldsymbol{F}_{EXT}(t_{n+1+\alpha}), \qquad (1)$$

where $\boldsymbol{M}$ is the consistent mass matrix, $\boldsymbol{C}$ is the viscous damping matrix, $\boldsymbol{a}$ is the algorithmic nodal acceleration vector, $\boldsymbol{v}$ is the algorithmic nodal velocity vector, $\boldsymbol{F}_{INT}$ is the internal nodal force vector, $\boldsymbol{F}_{EXT}$ is the external nodal force vector, $\boldsymbol{\sigma}$ is the vector of Cauchy stresses, $\alpha$ is the integration parameter of Hilber et al. (1977), and $t$ is time. Newmark's method can be used to update the algorithmic displacement and velocity vectors; in the nonlinear regime, Newton's method can be used to solve equation (1) iteratively.

In many cases, seismic waves propagate essentially in the vertical direction. The kinematical constraints imposed by vertically propagating waves are given by the conditions

$$\epsilon_{xx} = \epsilon_{yy} = \gamma_{xy} = 0\,, \qquad (2)$$

where $\epsilon_{xx}$ and $\epsilon_{yy}$ are the two horizontal normal strains, and $\gamma_{xy}$ is the shear strain on the horizontal plane $xy$. Special finite elements can be developed to satisfy these kinematical constraints. An example of a special finite element is a two-noded stick element with a linear displacement interpolation in the vertical $z$-direction as

$$u_i(t) = \sum_{A=1}^{2} N_A d_{Ai}(t)\,; \quad i = x, y, z\,. \qquad (3)$$

In can be seen that the spatial derivatives of $u_i$ as defined in (3) automatically satisfy the constraints imposed by vertically propagating waves.

A key ingredient of the FE model is a 3D bounding-surface plasticity theory with a vanishing elastic region (Borja and Amies 1994). The schematics of the constitutive model is shown in Fig. 1. Here, a soil is loaded uniaxially from an initially virgin condition denoted by point (a); it is then unloaded at point (c), and then reloaded back up at point (e). The elastic region is represented by the stress point $F$ itself, and is assumed to be infinitesimally small; consequently, plastic deformation takes place right at the onset of loading. The bounding surface, which is represented by a circular cylinder with a generating axis parallel to the hydrostatic axis, is free to translate on the $\pi$-plane; thus, hysteretic effects are captured naturally. The curvatures of the stress-strain curves are generated from an assumed exponential form of the plastic hardening modulus. By appropriate choice of parameters, the stress-strain curves can be made to replicate the variations of shear stiffness and damping ratio with shear strains. This constitutive model is based on total stresses, and hence is not capable of capturing the development of excess pore pressures due to cyclic loading (see Borja and Amies (1994) and Borja and Wu (1994) for further details of the model).

## ANALYSIS OF LOTUNG DHB DATA

Lotung is located in the southern part of the Lanyang plain in northeastern Taiwam, and is the site of two scaled-down nuclear plant containment structures (1/4-scale and 1/12-scale models) constructed by Electric Power Research Institute and Taiwan Power Company for soil-structure interaction research (Tang et al. 1990). On May 20, 1986, a magnitude 6.5 earthquake with an epicentral distance of 66 km and a focal depth of 15.8 km shook the test site. A downhole array (called DHB) located approximately at 49 m from the edge of the 1/4-scale model recorded nearly free-field motions at depths of 0, 6, 11, 17, and 47 m. In this section, these motions are analyzed using the proposed nonlinear FE model.

Previous studies on seismic wave propagation in Lotung indicated that the seismic waves of the May 20, 1986 event propagated nearly vertically, with only a 6°-angle of incidence (Chang et al. 1990). Hence, the model for vertical wave propagation described in the previous section may be used to analyze the Lotung problem. The FE mesh is composed of 47 stick finite elements for vertical wave propagation analysis. Borja and Chao (1995) demonstrated that this mesh can adequately capture the significant frequency contents of the recorded downhole motion in Lotung.

The following material parameters were used in the analysis (see Borja and Amies (1994) for further details): hardening function coefficient $h = 0.02\mu$; hardening function exponent $m = 1.5$; and plastic hardening modulus for bounding surface $H_0 = 0.6\mu$; where $\mu$ is the undegraded elastic shear modulus which varies with depth according to the variation of the shear wave velocity with depth as reported by Anderson and Tang (1989). These parameters automatically satisfy the observed variations of secant shear modulus and damping ratio with shear strains for the Lotung soil, as reported by Tang et al. (1990). Time integration is carried out with algorithmic parameters $\beta = 0.0325$, $\gamma = 0.60$, and $\alpha = -0.10$, at a constant time increment of $\Delta t = 0.02$ sec. A viscous, mass-proportional damping of 2 percent has been included in the dynamic equilibrium equation.

Partial results of the analysis are shown in Figs. 2–5. Here, the recorded east-west (EW), north-south (NS), and up-down (UD) accelerations at depth of 47 m were applied simultaneously at the base of the FE mesh. The effect of local soil condition is described by the downhole motions predicted by the model. The labels FA1–5, DHB6, DHB11, DHB17, and DHB47 were used in the original digitized recording, and pertain to stations at depths of 0, 6, 11, 17, and 47 m, respectively. Only the EW motions are compared in Figs. 2–5 for lack of space, but the analysis assumed the three components of motion to be fully coupled. Additional results for the remaining components of motion will be reported in a separate paper now under preparation.

Figure 2 compares the predicted and recorded EW downhole acceleration-time histories for array DHB, and shows that the model predicted the downhole responses with notable accuracy. The close agreement shown in Fig. 2 is noteworthy considering that the numerical model assumed coupled EW, NS, and UD motions, and confirms many crucial assumptions including the nearly zero angle of incidence of the seismic waves, the nearly free-field condition at the site, and the soil profile in the vicinity of this array.

To understand the importance of viscous damping on the predicted response, the viscous damping matrix $\boldsymbol{C}$ was set to zero and the analysis was repeated. Fig. 3 compares the predicted EW downhole acceleration-time histories, without viscous damping, with the recorded response for array DHB, and shows the predicted motion to lack the smoothness of the recorded response. Clearly, viscous damping is present in the recorded motion and may be attributed to local soft soil condition and the high water

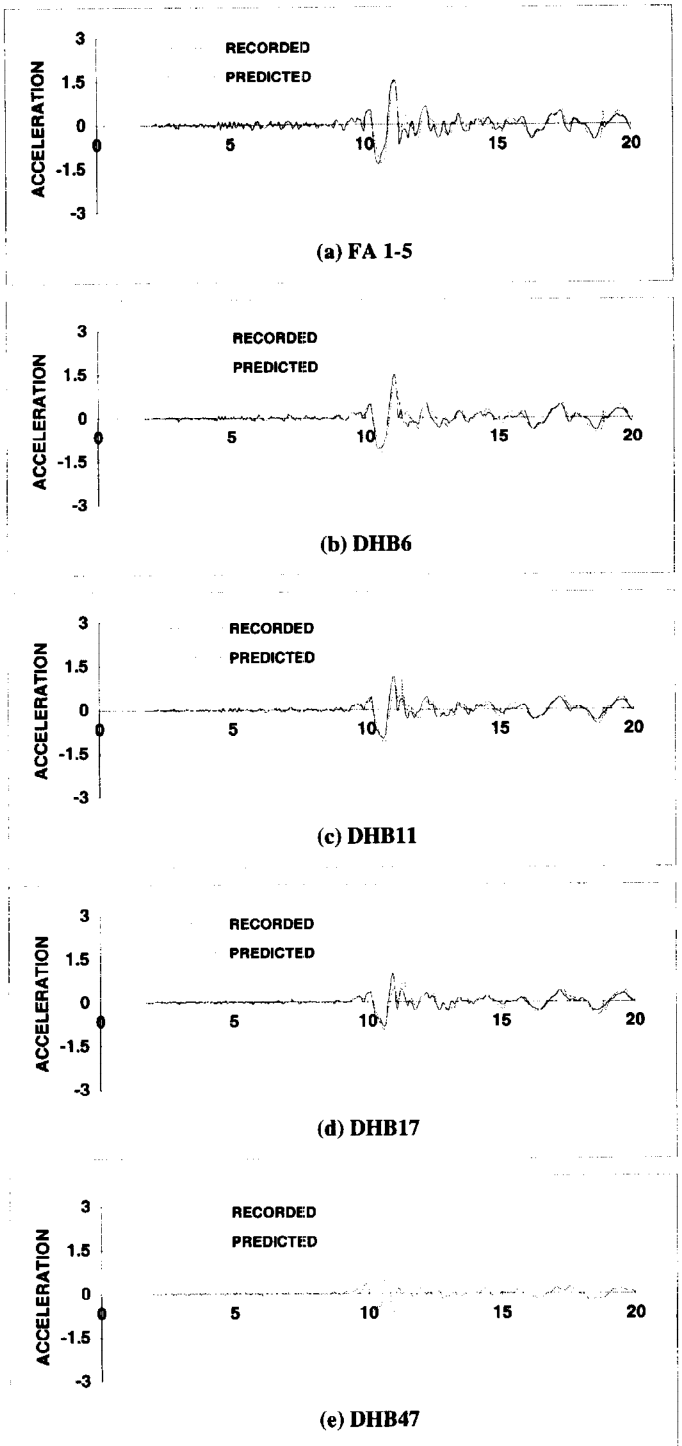


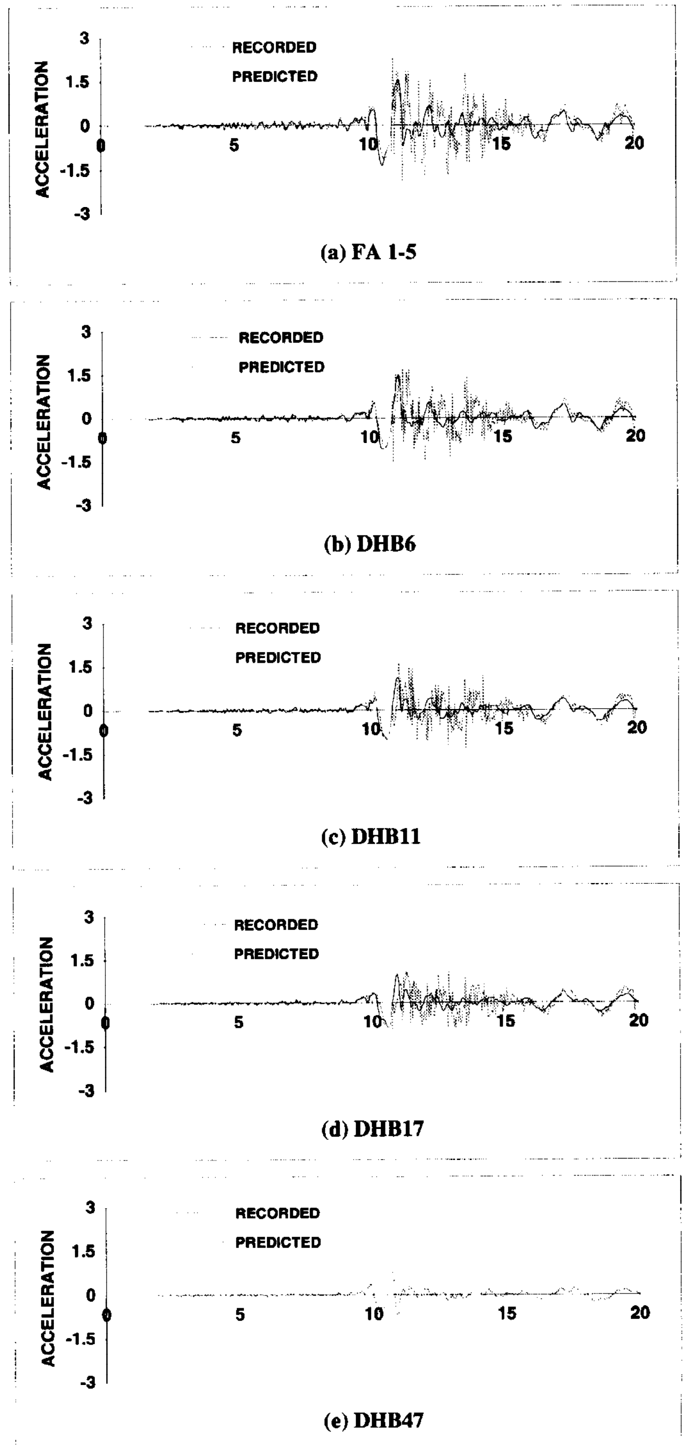


Figure 2. EW acceleration (m/sec$^2$) versus time (sec) histories of downhole motion for array DHB.

Figure 3. EW acceleration (m/sec$^2$) versus time (sec) histories of downhole motion for array DHB: no viscous damping.

table at the site.

To understand the importance of hysteretic damping on the predicted response, the plastic hardening function was set equal to infinity and the analysis was repeated. Since no hysteretic loop may form in a soil with an infinite plastic hardening modulus, hysteretic damping is suppressed altogether. Fig. 4 compares the predicted EW downhole acceleration-time histories, without hysteretic damping, with the recorded response for array DHB. The lack of agreement between the predicted and recorded responses

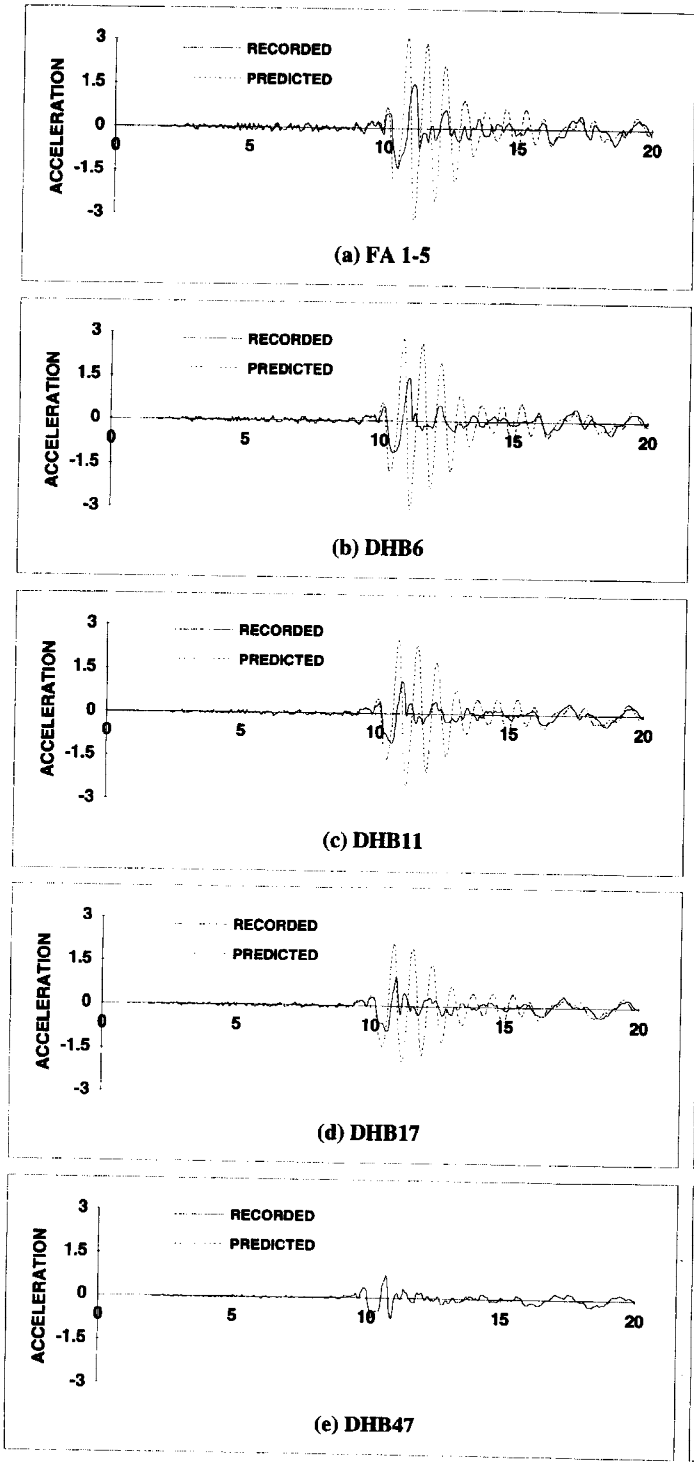


Figure 4. EW acceleration (m/sec$^2$) versus time (sec) histories of downhole motion for array DHB: no hysteretic damping.

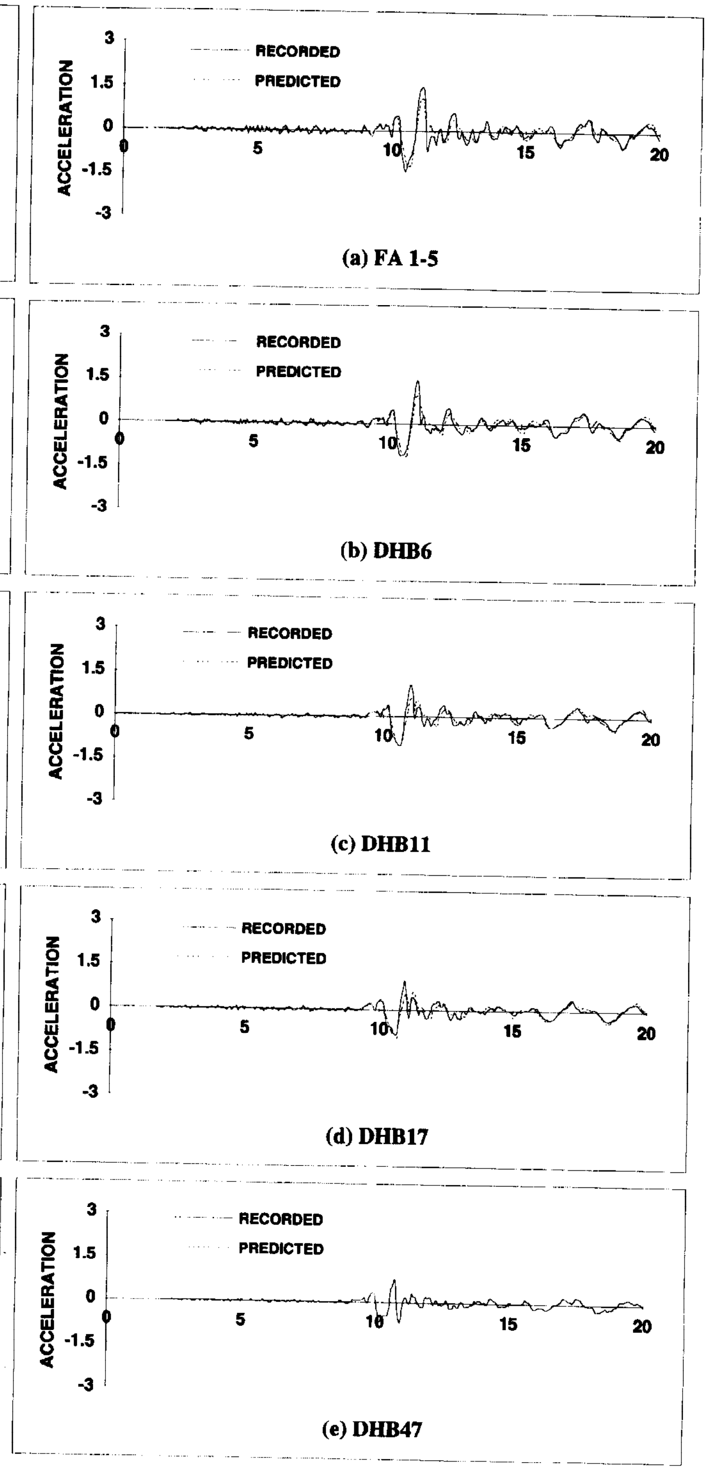


Figure 5. EW acceleration (m/sec$^2$) versus time (sec) histories of downhole motion for array DHB: no coupling of NS, EW and UD motions.

indicates that hysteretic damping and nonlinear material behavior are a significant component of the recorded response.

Finally, Fig. 5 compares the recorded and predicted EW acceleration-time histories of downhole motion assuming that the three components of motion were acting independently. In this case, the EW component of motion was generated using a one-dimensional wave propagation model. Clearly, the predicted motion differs from that shown in Fig. 2 and suggests that coupling effects are significant in the nonlinear regime. In other words, the one-dimensional wave propagation theory is not appropriate for problems which involve significant amount of plastic deformation.

## SUMMARY AND CONCLUSION

A nonlinear FE model for ground response analysis was developed to fully couple the three components of motion arising from plastic deformation effects. A 3D bounding surface plasticity theory with a vanishing elastic region allows these components of motion to be coupled naturally. The FE model was used to analyze the free-field downhole motion recorded by an array in Lotung, Taiwan during the earthquake of May 20, 1986. Results suggest that this seismic event was dominated by viscous, nonlinear soil behavior.

## ACKNOWLEDGMENTS

Financial support for this research was provided by National Science Foundation under Contract No. CMS-9114869, through Dr. C.J. Astill. The authors also acknowledge Dr. H.T. Tang and Electric Power Research Institute for making the digitized data for the Lotung site available.

## REFERENCES

Anderson, D.G. and Tang, Y.K. (1989). Summary of soil characterization program for the Lotung large-scale seismic experiment. *Proceedings of the EPRI/NRC/TPC Workshop on Seismic Soil-Structure Interaction Analysis Techniques Using Data from Lotung, Tawian EPRI NP-6154*, **1**, 4.1–4.20.

Borja, R.I. and Amies, A.P. (1994). Multiaxial cyclic plasticity model for clays." *J. of Geotech. Engrg.*, ASCE, **120**, 1051–1070.

Borja, R. I., and Wu, W. H. (1994), Vibration of foundations on incompressible soils with no elastic region. *J. Geotech. Engrg.*, ASCE, **120**, 1570–1592.

Borja, R. I., and Chao, H. Y. (1995). Nonlinear ground response analysis at Lotung array test site. *Proc. Pacific Conf. Earthquake Engrg.*, Melbourne, Australia, Nov. 20–22.

Chang, C.Y., Mok, C.M., Power, M.S., Tang, Y.K., Tang, H.T., and Stepp, J.C. (1990). "Equivalent linear and nonlinear ground response analyses at Lotung seismic experiment site." *Proceedings of Fourth U.S. National Conference on Earthquake Engineering*, Palm Springs, California, 1, 327–336.

Hilber, H.M., Hughes, T.J.R. and Taylor, R.L. (1977). Improved numerical dissipation for time integration algorithms in structural dynamics. *Earthquake Engrg Struct. Dyn.*, **5**, 283–292.

Kausel, E. and Roësset, J.M. (1984). Soil amplification: some refinements. *Soil Dyn. and Earthquake Engrg.*, **3**, 116–123.

Schnabel, P.B. et al. (1972). *SHAKE—A computer program for earthquake response analysis of horizontally layered sites*, Report No. UCB/EERC 72-12, University of California, Berkeley.

Seed, H.B. and Idriss, I.M. (1969). Influence of soil conditions on ground motions during earthquakes. *J. Soil Mech. Found. Div.*, ASCE, **95**, 99–137.

Tang, H.T., Tang Y.K. and Stepp, J.C. (1990). Lotung large-scale seismic experiment and soil-structure interaction method validation, *Nuclear Engineering and Design*, **123**, 197–412.